

Dynamics of a planar vortex filament under the quantum local induction approximation

Robert A. Van Gorder*

Department of Mathematics, University of Central Florida, Orlando, FL 32816-1364 USA

*Corresponding author. Email: rav@knights.ucf.edu

September 17, 2014

Abstract

The Hasimoto planar vortex filament is one of the rare exact solutions to the classical local induction approximation (LIA). This solution persists in the absence of friction or other disturbances, and it maintains its form over time. As such, the dynamics of such a filament have not been extended to more complicated physical situations. We consider the planar vortex filament under the quantum LIA, which accounts for mutual friction and the velocity of a normal fluid impinging on the filament. We show that, for most interesting situations, a filament which is planar in the absence of mutual friction at zero temperature will gradually deform due to friction effects and the normal fluid flow corresponding to warmer temperatures. The influence of friction is to induce torsion, so the filaments bend as they rotate. Furthermore, the flow of a normal fluid along the vortex filament length will result in a growth in space of the initial planar perturbations of a line filament. For warmer temperatures, these effects increase in magnitude, since the growth in space scales with the mutual friction coefficient. A number of nice qualitative results are analytical in nature, and these results are verified numerically for physically interesting cases.

Keywords: Vortex dynamics; vortex filament; superfluid dynamics; integrable models

PACS: 67.25.dk, 67.25.dg, 02.30.Ik, 47.32.C-

1 Introduction

Superfluid He II has been viewed hydrodynamically as a mixture of two components [1], consisting of a superfluid liquid moving with a velocity \mathbf{v} and a classical fluid. This superfluid component has no shear viscosity and cannot absorb or carry heat. The motion of the two components is thermodynamically reversible and therefore they are independent. Due to the appearance of quantized vortices, the model fails in general [2, 3]. The HVBK model (Hall-Vinen-Bekarevich-Khalatnikov model) [4, 5, 6] describes the coarse-grained (average) hydrodynamics of superfluids containing a mass of nearly parallel vortex lines. For a modern review of these issues, see [7].

The motion of a single quantized vortex filament is governed by non-local Biot-Savart dynamics. These non-local dynamics are often approximated through the local induction approximation (LIA). We should note that a planar vortex filament solution is known to exist for the classical local induction approximation (LIA). For these reasons, it makes sense to consider the Schwarz [8] model

for the dynamics due to the velocity \mathbf{v} , and this model is given by

$$\mathbf{v} = \gamma \kappa \mathbf{t} \times \mathbf{n} + \alpha \mathbf{t} \times (\mathbf{U} - \gamma \kappa \mathbf{t} \times \mathbf{n}) - \alpha' \mathbf{t} \times (\mathbf{t} \times (\mathbf{U} - \gamma \kappa \mathbf{t} \times \mathbf{n})). \quad (1)$$

which approximates the non-locality of the Biot-Savart dynamics with the local LIA term $\gamma \kappa \mathbf{t} \times \mathbf{n}$, while also accounting for mutual friction. We refer to (1) as a quantum LIA. The vector \mathbf{U} is the dimensionless normal fluid velocity, \mathbf{t} and \mathbf{n} are the unit tangent and unit normal vectors to the vortex filament, κ is the local curvature, $\gamma = \Gamma \ln(c/\hat{\kappa}a_0)$ is a dimensionless composite parameter (Γ is the dimensionless quantum of circulation, c is a scaling factor of order unity, $a_0 \approx 1.3 \times 10^{-8}$ is the effective core radius of the vortex, $\hat{\kappa}$ is the average curvature), α and α' are dimensionless mutual friction coefficients which are small (except near the λ -point; for reference, the λ -point is the temperature (which at atmospheric pressure is $\approx 2.17\text{K}$) below which normal fluid Helium transitions to superfluid Helium[9]). The friction parameters α and α' are small, and Table 1 of Schwarz [8] shows that at temperature $T = 1\text{K}$ we have $\alpha = 0.006$ and $\alpha' = 0.003$, while at temperature $T = 1.5\text{K}$ we have $\alpha = 0.073$ and $\alpha' = 0.018$. The other coefficients in the quantum LIA are often taken to be of order unity. In the limit $(\alpha, \alpha') \rightarrow (0, 0)$, we recover the classical Da Rios equations for the motion of a vortex filament in a standard fluid [10, 11]:

$$\mathbf{v} = \gamma \kappa \mathbf{t} \times \mathbf{n}, \quad (2)$$

which is just the classical LIA. Including the γ term in the timescale, (3) can be written as

$$\mathbf{v} = \kappa \mathbf{t} \times \mathbf{n} + \alpha \mathbf{t} \times (\mathbf{V} - \kappa \mathbf{t} \times \mathbf{n}) - \alpha' \mathbf{t} \times (\mathbf{t} \times (\mathbf{V} - \kappa \mathbf{t} \times \mathbf{n})), \quad (3)$$

where $\mathbf{V} = \frac{1}{\gamma} \mathbf{U}$.

Regarding the classical fluid LIA, Hasimoto [12] considered a planar vortex filament in the curvature-torsion frame of reference. This influential and often cited paper demonstrates the relation between the curvature of a vortex filament and elastica. Such a solution was also considered by Kida [13], who obtained results in terms of elliptic integrals in the moving (time-dependent) arc length coordinate frame, with stability results for some filaments in this framework later provided [14]. Fukumoto [15] considered the influence of background flows on such vortex filaments. In the Cartesian coordinate frame, some preliminary results were determined in Van Gorder [16], though only some special solutions were given. Using a multiple-scales approach, perturbation solutions were constructed in the Cartesian reference frame by Van Gorder [17], as a function of the maximal deflection from the reference axis. These perturbation solutions were accurate provided that deviations from a reference axis were sufficiently bounded. Orbital stability of the planar filament was discussed in Van Gorder [18] through an analytical approach. There is an alternate formulation of the classical LIA, given by Umeki [19], which provides the LIA in an arclength-tangent vector coordinate frame. The Hasimoto filament can be determined exactly in this frame (as is also true of the curvature-torsion frame), and the results were worked out by Van Gorder [20]. However, the conversion between the arc-length and Cartesian solutions is not simple, so it is often worthwhile to consider the Cartesian case directly.

While the planar filament has been studied under multiple models, for quantum LIA such filaments have so far been approximated (numerically or analytically) under potential forms of the LIA (such as in Cartesian coordinates [21] or in the arclength-tangent vector frame [22]). These are approximations to the LIA, valid under certain restrictions such as that deviations from a reference axis must remain small to be of sufficient bounded variation, and thus a more direct

approach could be enlightening. In particular, while such potential formulations are useful in some parameter regimes, there are often restrictions (such as on amplitude of any waves along a filament, on the wave number of solutions, and so on) that must be obeyed. In the present paper, we work directly with the LIA, as opposed to any approximating potential form. While this means that the mathematics may not be as elegant, we benefit from having a precise representation of the solutions. We shall consider the quantum LIA directly in Cartesian coordinates, since this allows for easy visualization of the vortex filament solutions. Our goal in doing this is to determine both qualitative and quantitative effects of the mutual friction parameters and the normal fluid velocity on the planar vortex filaments. In this way, we extend the planar filaments of Hasimoto valid under the classical LIA to a new type of filament under the quantum form of the LIA.

The paper is organized as follows. In Section 2, we review the planar filament in the classical fluid model, and attempt to extend such a solution to the quantum fluid model directly. A solution of this type is possible only when the normal fluid velocity varies in space and takes a particular form, meaning that such a solution is of narrow applicability. In Section 3, we overcome such difficulties by defining a different type of filament, which happens to be planar at $\alpha, \alpha' = 0$ yet non-planar away from the origin when $\alpha, \alpha' > 0$. Such a solution is the true generalization of the planar filament for the quantum LIA, and indeed this solution allows us to study the dynamics of a planar filament in the quantum LIA. The influence of the normal fluid velocity and of the mutual friction parameters on this family of solutions is discussed both through analytical approximation and numerical simulation. The results suggest that the friction parameters result in a twisting of the filaments, while the normal fluid directed along the filament results in a type of growth in the space variable, reminiscent of (but different than) the Donnelly - Glaberson instability [23, 24, 25] for helical filaments under the quantum LIA.

2 A purely planar vortex filament

In the Cartesian coordinate geometry, we write $\mathbf{r} = (x, y, z)$. Then, in this coordinate frame we have [17]

$$\mathbf{t} = \frac{d\mathbf{r}}{ds} = \frac{d\mathbf{r}}{dx} \frac{dx}{ds} = (1, y_x, z_x) \frac{dx}{ds} \quad (4)$$

and

$$\mathbf{v} = \mathbf{r}_t = (0, y_t, z_t), \quad (5)$$

where

$$\frac{dx}{ds} = \frac{1}{\sqrt{1 + y_x^2 + z_x^2}}. \quad (6)$$

We then have

$$\begin{aligned} \kappa \mathbf{n} &= \frac{d\mathbf{t}}{ds} = \frac{d\mathbf{t}}{dx} \frac{dx}{ds} \\ &= -(y_x y_{xx} + z_x z_{xx}) \frac{dx}{ds} \mathbf{i}_x + [y_{xx} z_x - y_x z_x z_{xx} + y_{xx}] \frac{dx}{ds} \mathbf{i}_y + [z_{xx} y_x^2 - z_x y_x y_{xx} + z_{xx}] \frac{dx}{ds} \mathbf{i}_z. \end{aligned} \quad (7)$$

The general form of a rotating planar vortex filament under LIA is given by

$$\mathbf{r}(x, t) = (x, \cos(t)\psi(x), -\sin(t)\psi(x)), \quad (8)$$

where ψ is some unknown function to be determined. Note that the solution lies on a plane which intersects the x -axis and rotates in time around the x -axis. We shall be most interested in a normal fluid velocity vector oriented along the vortex filament, $\mathbf{V} = (V, 0, 0)$, since this will often drive Kelvin waves along the filament.

Placing the solution representation (8) into the classical LIA (2), and making use of (4)-(7), we find that

$$\kappa \mathbf{t} \times \mathbf{n} = (0, \sin(t), \cos(t)) \frac{\psi''}{(1 + \psi'^2)^{3/2}} \quad (9)$$

while

$$\mathbf{v} = \mathbf{r}_t = (0, -\sin(t), -\cos(t))\psi(x). \quad (10)$$

Therefore, (8) is a solution to the classical LIA provided that

$$\psi + \frac{\psi''}{(1 + \psi'^2)^{3/2}} = 0. \quad (11)$$

If we carry out similar computations for the quantum LIA (3), and set all three components of the resulting vectors equal, we shall find

$$0 = -\alpha \frac{\psi' \psi''}{(1 + \psi'^2)^2} + \alpha' V \frac{\psi'^2}{1 + \psi'^2}, \quad (12)$$

$$\sin(t)\psi = -\sin(t) \left\{ \frac{(1 - \alpha')\psi''}{(1 + \psi'^2)^{3/2}} - \frac{\alpha V \psi'}{(1 + \psi'^2)^{1/2}} \right\} - \cos(t) \left\{ \frac{\alpha \psi''}{(1 + \psi'^2)^2} - \frac{\alpha' V \psi'}{1 + \psi'^2} \right\}, \quad (13)$$

$$-\cos(t)\psi = \cos(t) \left\{ \frac{(1 - \alpha')\psi''}{(1 + \psi'^2)^{3/2}} - \frac{\alpha V \psi'}{(1 + \psi'^2)^{1/2}} \right\} - \sin(t) \left\{ \frac{\alpha \psi''}{(1 + \psi'^2)^2} - \frac{\alpha' V \psi'}{1 + \psi'^2} \right\}, \quad (14)$$

where $V = U/\gamma$. Each of these equations has a term which we assume is zero:

$$\frac{\alpha \psi''}{(1 + \psi'^2)^2} - \frac{\alpha' V \psi'}{1 + \psi'^2}. \quad (15)$$

This term naturally vanishes in the $\alpha, \alpha' \rightarrow 0$ limit. Meanwhile, the analogue to (11) in the quantum case is apparently

$$\psi + \frac{(1 - \alpha')\psi''}{(1 + \psi'^2)^{3/2}} - \frac{\alpha V \psi'}{(1 + \psi'^2)^{1/2}} = 0. \quad (16)$$

Let us assume that (15) holds equal to zero. This would then imply that (16) takes the form

$$\psi + \left(1 - \alpha' - \frac{\alpha^2}{\alpha'}\right) \frac{\psi''}{(1 + \psi'^2)^{3/2}} = 0. \quad (17)$$

Let $\hat{\psi}(x)$ be a bounded and periodic solution of (11). Then, the scaling

$$\psi(x) = \sqrt{1 - \alpha' - \frac{\alpha^2}{\alpha'}} \hat{\psi} \left(\frac{x}{\sqrt{1 - \alpha' - \alpha^2/\alpha'}} \right) \quad (18)$$

is a solution of (17). This provides a nice link between the classical and quantum LIA solutions, and shows that a purely planar solution is possible, provided that the consistency term (15) vanishes.

That said, the consistency term (15) does not, in general vanish. To see why, note that a planar filament solution to (11) is periodic. On the other hand, let us rescale the coefficients in (15) to obtain the differential equation

$$h'' = h' + h'^3. \quad (19)$$

After obtaining a first integral, we should have

$$h' = \pm \frac{1}{\sqrt{Ce^{-2x} - 1}}, \quad (20)$$

and therefore at some finite value of x , h should become singular. Since this is incompatible with a planar solution, we conclude that (15) does not vanish when ψ is a bounded and periodic function as given in (18). Note that a solution (18) may still remain a very good approximation to a true filament solution. In this case, the consistency term should be sufficiently small. Indeed, the consistency term is of order α , whereas the solution (18) is determined by an equation of order unity.

There is a fix that allows us to obtain a solution (18) while also satisfying the consistency condition (15), but this involves picking the normal fluid velocity in a very specific way. In particular, if instead of considering a constant velocity for the normal fluid flow, we were to pick $\mathbf{V} = (V(x), 0, 0)$, then we can use (15) to determine conditions on such a function $V(x)$. Doing so, one finds

$$V(x) = \frac{\alpha}{\alpha'} \frac{\psi''}{\psi'(1 + \psi'^2)}. \quad (21)$$

While this is, of course, a rather narrow restriction on the form of \mathbf{V} , it does permit a very elegant solution (18). Physically, this restriction is even more limiting, since such a form for $V(x)$ means that \mathbf{V} would not satisfy the continuity equation for an incompressible fluid.

As it turns out, a purely planar vortex filament moving without change in form is simply too specialized to exist in a superfluid under normal conditions (the exact solution we get when $V = V(x)$ takes a specific form is certainly not what one would call general in any sense). Rather, it makes more sense to consider a family of vortex filaments that generalize the planar filament in the sense that they reduce to the planar filament in the limit $\alpha, \alpha' = 0$. For $\alpha, \alpha' > 0$, such filaments would not be confined to a plane which rotates about the reference axis, but would rather exhibit planar behavior in a local sense, while exhibiting other behaviors asymptotically for large $|x|$. In a way, we could view such vortex filaments as deformations of the planar filaments, with the deformations due to the influence of both the mutual friction parameters and the normal fluid velocity.

3 Deformation of a planar filament due to superfluid parameters

When attempting to construct a purely planar quantum generalization of the planar filament found in the classical LIA, we saw in Section 2 that in most cases (for instance, when \mathbf{V} is a constant vector) there are too few degrees of freedom if we assume that the time evolution of the vortex filament follows (8). In order to obtain the most useful generalization of the classical planar filament, we need to consider that the superfluid parameters can cause the filament to become non-planar in a variety of ways. Spatial growth of waves along a quantum vortex filament is possible, while

modified torsion due to the mutual friction parameters is also an issue. To account for such effects, we propose a solution of the form

$$\mathbf{r}(x, t) = (x, \cos(t)\phi(x) + \sin(t)\psi(x), \cos(t)\psi(x) - \sin(t)\phi(x)). \quad (22)$$

Placing (22) in (3), we obtain the differential equations

$$\begin{aligned} \phi + \frac{(1 - \alpha')\phi''}{(1 + \phi'^2 + \psi'^2)^{3/2}} + \frac{\alpha\psi''}{(1 + \phi'^2 + \psi'^2)^2} - \frac{\alpha V\phi'}{(1 + \phi'^2 + \psi'^2)^{1/2}} \\ - \frac{\alpha'V\psi'}{(1 + \phi'^2 + \psi'^2)} - \frac{\alpha\phi'(\psi'\phi'' - \phi'\psi'')}{(1 + \phi'^2 + \psi'^2)^2} = 0, \end{aligned} \quad (23)$$

$$\begin{aligned} \psi + \frac{(1 - \alpha')\psi''}{(1 + \phi'^2 + \psi'^2)^{3/2}} - \frac{\alpha\phi''}{(1 + \phi'^2 + \psi'^2)^2} - \frac{\alpha V\psi'}{(1 + \phi'^2 + \psi'^2)^{1/2}} \\ + \frac{\alpha'V\phi'}{(1 + \phi'^2 + \psi'^2)} - \frac{\alpha\psi'(\psi'\phi'' - \phi'\psi'')}{(1 + \phi'^2 + \psi'^2)^2} = 0. \end{aligned} \quad (24)$$

By including two unknown functions, we obtain two differential equations for two unknown functions, as opposed to two differential equations for one unknown function (as was the case for the purely planar filament). The motion of the filament (22) is not purely planar, though it contains the pure planar filament as a reduction (taking $\psi \rightarrow 0$ gives the pure planar filament).

Equations (23)-(24) come from balancing the last two components in the vector equation resulting from the assumption (22). Since the solution is no longer purely planar, the x -component of this equation is not identically zero, and is given in terms of ϕ and ψ by

$$J[\phi, \psi] = (1 - \alpha') \frac{(\psi''\phi' - \psi'\phi'')}{(1 + \phi'^2 + \psi'^2)^{3/2}} - \alpha \frac{(\phi'\phi'' + \psi'\psi'')}{(1 + \phi'^2 + \psi'^2)^2} + \alpha'V \frac{\phi'^2 + \psi'^2}{1 + \phi'^2 + \psi'^2}. \quad (25)$$

The assumption (22) is then reasonable when the quantity $J[\phi, \psi]$ is sufficiently small, and therefore we have a consistency condition of the form $J[\phi, \psi] \sim \epsilon$ where ϵ is sufficiently small. If the amplitude of the solution (22) is small enough, then this quantity will be rather small. In the numerical solutions considered later, we shall see that $J[\phi, \psi] \sim \alpha^2$. Therefore, the solutions under the approximation (22) are reasonable up to order α corrections.

Since we should have a planar filament when $\alpha, \alpha' \rightarrow 0$, we should take ϕ to be of order unity and ψ to be of order α . While a complete analytical analysis of (23)-(24) is not possible since the equations are too complicated, we can make some qualitative observations. If we assume $\psi = \alpha\Psi$ for some function Ψ of order unity, and we neglect order α^2 and higher terms, we should have

$$\phi + \frac{(1 - \alpha')\phi''}{(1 + \phi'^2)^{3/2}} - \frac{\alpha V\phi'}{(1 + \phi'^2)^{1/2}} = 0, \quad (26)$$

$$\Psi + \frac{(1 - \alpha')\Psi''}{(1 + \phi'^2)^{3/2}} - \frac{\alpha V\Psi'}{(1 + \phi'^2)^{1/2}} = \frac{\phi''}{(1 + \phi'^2)^2} - \frac{\alpha'V}{\alpha} \frac{\phi'}{1 + \phi'^2}. \quad (27)$$

While simplified from (23)-(24), these equations are still too complicated to solve exactly, owing to the fact that (26) does not have a first integral for $\alpha \neq 0$. In the case where the amplitude A of a solution ϕ is sufficiently small, we should find

$$\phi(x) = A \cos\left(\frac{\sqrt{4(1 - \alpha') - \alpha^2 V^2}}{2(1 - \alpha')}x\right) \exp\left(\frac{\alpha V}{2(1 - \alpha')}x\right) + O(A^3). \quad (28)$$

For small A , the order A^3 corrections are negligible. Near the origin, the solutions maintain a planar appearance, since the exponential growth or decay rate is of order α . The solutions will grow in the space variable for either $x > 0$ or $x < 0$, depending on the sign of V . So, there is growth driven by the normal fluid along the direction in which the normal fluid points. This is analogous to the Donnelly - Glaberson instability seen when a normal fluid flow is directed along a helical vortex filament. Note that, in the case where ϕ is of order unity and ψ is of order α , we find that the consistency condition (25) is of order α^2 , meaning that such solutions are valid to order α . Since $\alpha' < \alpha \ll 1$, this is still a reasonably good approximation.

It is possible to exploit the symmetry of equations (23)-(24) to obtain a single complex equation. Defining $W = \phi + i\psi$, and adding i times (24) to (23), we obtain

$$W + \frac{(1 - \alpha')W''}{(1 + |W'|^2)^{3/2}} - \frac{\alpha V W'}{(1 + |W'|^2)^{1/2}} + i \left\{ \frac{\alpha' V W'}{1 + |W'|^2} - \frac{\alpha W''}{(1 + |W'|^2)^2} - \frac{\alpha}{2} \frac{W'(W'^* W'' - W' W''^*)}{(1 + |W'|^2)^2} \right\} = 0. \quad (29)$$

Here, $*$ denotes complex conjugation. Note that (29) implies that (23)-(24) can be mapped to a three-dimensional real system, despite the fact that (23)-(24) is a four-dimensional real dynamical system. This is due to a certain type of symmetry that exists in the equations (23)-(24) which is inherited from the LIA itself. To demonstrate this, let us consider the representation $W(x) = R(x) \exp(i \int_0^x \theta(\sigma) d\sigma)$, where R and θ are real-valued functions. Placing this representation into (29), and separating the resulting equation into real and imaginary parts, we obtain

$$R + \frac{(1 - \alpha')(R'' - R\theta^2)}{(1 + R'^2 + R^2\theta^2)^{3/2}} + \frac{\alpha(2R'\theta + R\theta')}{(1 + R'^2 + R^2\theta^2)^2} - \frac{\alpha V R'}{(1 + R'^2 + R^2\theta^2)^{1/2}} - \frac{\alpha' V R\theta}{(1 + R'^2 + R^2\theta^2)} + \frac{\alpha R'[(2R'^2 - RR'')\theta + R^2\theta^2 + RR'\theta']}{(1 + R'^2 + R^2\theta^2)^2} = 0, \quad (30)$$

$$\frac{(1 - \alpha')(2R'\theta + R\theta')}{(1 + R'^2 + R^2\theta^2)^{3/2}} - \frac{\alpha(R'' - R\theta^2)}{(1 + R'^2 + R^2\theta^2)^2} - \frac{\alpha V R\theta}{(1 + R'^2 + R^2\theta^2)^{1/2}} + \frac{\alpha' V R'}{(1 + R'^2 + R^2\theta^2)} + \frac{\alpha R\theta[(2R'^2 - RR'')\theta + R^2\theta^2 + RR'\theta']}{(1 + R'^2 + R^2\theta^2)^2} = 0. \quad (31)$$

Equations (30)-(31) constitute a three-dimensional dynamical system. This system can be solved provided that it is non-degenerate. Writing the system in the form

$$[(1 - \alpha')\sqrt{1 + R'^2 + R^2\theta^2} - \alpha R R'\theta]R'' + \alpha R(1 + R'^2)\theta' = F_1(R, R', \theta), \quad (32)$$

$$-\alpha(1 + R^2\theta^2)R'' + [(1 - \alpha')R\sqrt{1 + R'^2 + R^2\theta^2} + \alpha R^2 R'\theta]\theta' = F_2(R, R', \theta), \quad (33)$$

for appropriately defined F_1 and F_2 . The determinant of the Jacobian of the left hand side of (32)-(33) must not vanish, which is equivalent to the condition

$$(1 + \alpha')R(1 + R'^2 + R^2\theta^2) + \alpha^2 R(1 + R^2\theta^2) \neq 0. \quad (34)$$

In the limit $\alpha, \alpha' \rightarrow 0$, this condition becomes

$$R(1 + R'^2 + R^2\theta^2) \neq 0. \quad (35)$$

Therefore, given small enough α and α' , the system (30)-(31) is non-degenerate, and a solution does exist.

Equations (30)-(31) are no simpler to study than (23)-(24). However, let us assume that any deviations from the reference axis are small, so that $|R| \leq \epsilon \ll 1$. Let us also define the function $\xi(x) = R'(x)/R(x)$, which itself should be of order unity. Then, neglecting terms of order ϵ^2 and higher, equations (30)-(31) are reduced to

$$1 + (1 - \alpha')(\xi' + \xi^2 - \theta^2) + \alpha(2\xi\theta + \theta') - \alpha V\xi - \alpha' V\theta = 0, \quad (36)$$

and

$$(1 - \alpha')(2\xi\theta + \theta') - \alpha(\xi' + \xi^2 - \theta^2) - \alpha V\theta + \alpha' V\xi = 0, \quad (37)$$

respectively. To study the qualitative effects of the remaining nonlinearity, we set $V = 0$, which is physically relevant in the low-temperature limit and also in the case of superfluid Helium 3. We obtain

$$\beta + 2\xi\theta + \theta' = 0, \quad (38)$$

$$\beta' + \xi' + \xi^2 - \theta^2 = 0, \quad (39)$$

where

$$\beta = \frac{\alpha}{\alpha^2 + (1 - \alpha')^2} \quad \text{and} \quad \beta' = \frac{1 - \alpha'}{\alpha^2 + (1 - \alpha')^2}. \quad (40)$$

This system admits two equilibrium points when $\beta > 0$: $(\xi^*, \theta^*) = (-\beta/(2\nu), \nu)$ and $(\xi^*, \theta^*) = (\beta/(2\nu), -\nu)$, where

$$\nu = \sqrt{\frac{\beta' + \sqrt{\beta'^2 + \beta^2}}{2}}. \quad (41)$$

A linear stability analysis shows that the equilibrium $(-\beta/(2\nu), \nu)$ is unstable, whereas $(\beta/(2\nu), -\nu)$ is linearly stable. Eigenvalues of the Jacobian for system (38)-(39) take the form $\lambda_{\pm} = \frac{\beta}{\theta^*} \pm 2i\theta^*$, so the stable solutions should spiral inward toward the equilibrium, while the unstable solutions should spiral outward from the equilibrium, in the (ξ, θ) phase space. If we consider the space-reversal, the equilibrium points switch stability properties. This suggests that on one half of the x -axis, the perturbations along the vortex filament decay, whereas for the opposite half of the x -axis such perturbations grow in space.

From the analysis above, we draw several conclusions about the deformation of a planar vortex filament in the quantum form of the LIA. First, the effect of V , the scaled normal fluid velocity, is to grow the planar wave in amplitude along the direction which the normal fluid velocity vector is pointing. The rate of growth in space is moderated by the friction parameter α , which is small. The smaller the parameter α , the slower the growth in space (in the perturbative limit). The inclusion of mutual friction parameters results in a non-trivial phase term, θ . This feature implies that there are torsion effects not present in the classical planar filament. If the initial condition is $\theta(0) = 0$, then such effects are small near the origin, but can become large for large values of $|x|$. These are all behaviors that are absent in the classical planar filament, but which are suggested by the mathematics above in the case of a quantum planar filament.

In order to verify some of the behaviors suggested by the analytics above, we turn to numerical solutions. Since (30)-(31) are non-degenerate and are equivalent to (23)-(24), a solution pair $(\phi(x), \psi(x))$ exists (at least locally) for reasonable values of α, α' and V . We find that the standard

RKF-45 method is sufficient to numerically approximate the solutions of (23)-(24) to a desirable accuracy. When $\psi(x) \equiv 0$, we obtain the classical planar vortex filament solution. Therefore, the initial condition $\psi(0) = 0$ makes sense. We take $\phi(0) > 0$ to be the distance of the planar filament from the reference axis at the origin. Conditions $\phi'(0) = \psi'(0) = 0$ are not required, but they enforce a nice local symmetry at the origin.

In Figure 1, we consider the planar filament in the $T = 1\text{K}$ case in the presence of a normal fluid velocity directed along the positive x -axis. We also plot the $J[\phi, \psi]$ term given in (25). This term is zero when the vortex filament is purely planar. For our approximation (22) to be reasonable, the term $J[\phi, \psi]$ should be small. As we see in Figure 2, this term is roughly of the order α^2 . Therefore, for small enough α the assumption of purely rotational motion given in (22) is reasonable. In Figures 3 and 4 we do the same for the $T = 1.5\text{K}$ case. Growth in space of waves along the line filament occur much more rapidly when temperature increases, since α increases and hence the combined term αV increases - resulting in more exponential growth.

The numerical simulations suggest that the planar filaments do grow with the space variable due to the normal fluid flow, and that the direction of the normal fluid flow along the filament determines where this growth takes place. This is shown nicely when comparing Figures 2 and 3, which model the same situation only with the direction of \mathbf{V} reversed. Numerical results also show that the greater the speed of the normal fluid, the greater the growth. Both the direction and rate of growth (as a function of temperature and normal fluid velocity) are in agreement with the qualitative analysis performed above. In particular, this is in complete agreement with what was suggested by the analytical approximation in the small-amplitude limit, (28). The rate of growth in space is greater when α is larger, hence the planar filaments deviate from the reference axis by a larger extent in warmer temperatures.

Near the origin, the solutions all appear planar in form. However, for larger values of $|x|$, the solutions undergo torsion effects due to the interaction with the fluid modeled by the mutual friction parameters, α and α' . This is best seen when we compare a true planar filament solution to the classical LIA ($\alpha, \alpha' = 0$) with one of the quantum vortex filaments. We do this in Figure 5, where we see that close to the origin the two filaments agree, whereas as one gets further from the origin, the effects of the mutual friction parameters result in a bending of the rotating filament, while the influence of the normal fluid velocity causes growth in space. For negative x , the quantum filament eventually takes on a helical form, which contrasts with the planar form of the classical filament. For positive x , the quantum filament undergoes strong growth.

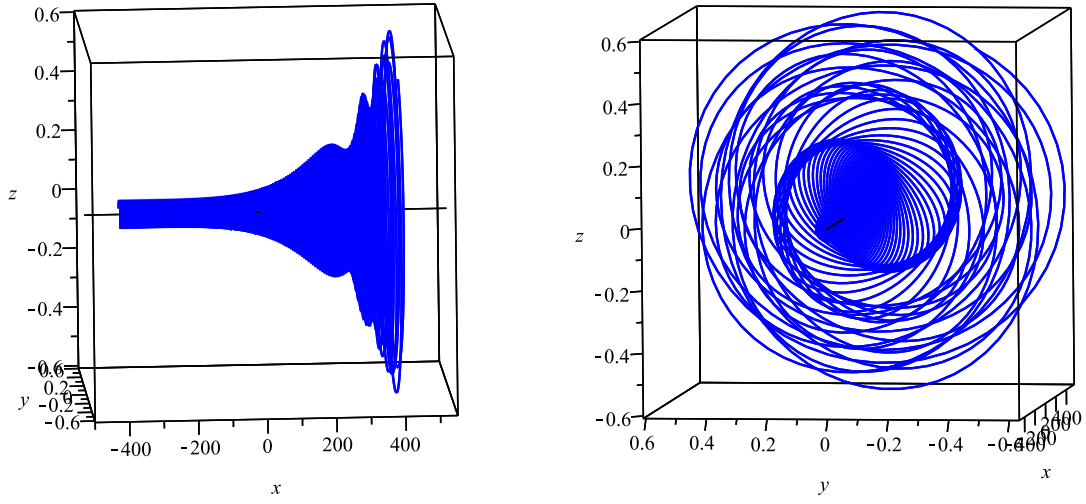


Figure 1: (Color Online) Two views of the deformed planar filament described by (22) when the temperature of the superfluid is $T=1K$ ($\alpha = 0.006$, $\alpha' = 0.003$) and $V = 1$. The filament is given by numerically solving (23)-(24) subject to $\phi(0) = 0.1$, $\psi(0) = 0$, $\phi'(0) = 0$, $\psi'(0) = 0$. The x -axis is given by a solid black line. It is clear that the solutions grow in the space variable, in the direction of $\mathbf{V} = (V, 0, 0)$. If we were to select $V < 0$, the growth would be directed along the negative x -axis.

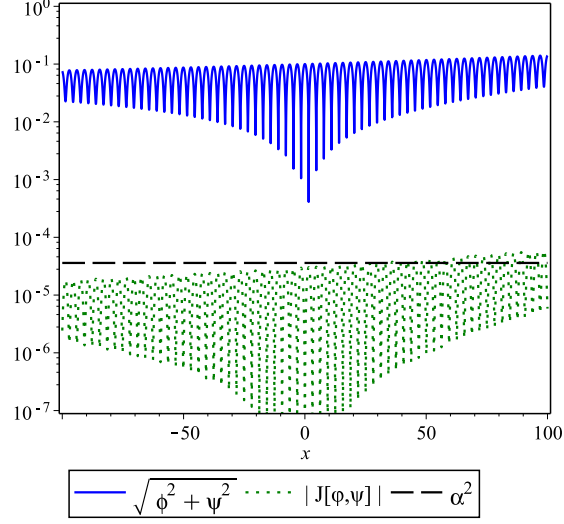


Figure 2: (Color Online) Plot of the error term $J[\phi, \psi]$ over x , along with the norm $\sqrt{\phi^2 + \psi^2}$, for the T=1K case. The value of $\sqrt{\phi^2 + \psi^2}$ is a measure of the deviation of the filament from the x -axis. This function oscillates with a maximal value of the order 10^{-1} to 10^0 , whereas the error due to neglecting non-rotational motion (due to the assumption of a solution of the form (22)) scales near 10^{-5} . This is consistent with the observation that $J[\phi, \psi] = O(\alpha^2)$. To see this, we also plot α^2 for our choice of $\alpha = 0.006$. What this shows is that the magnitude of the deflections from the x -axis are orders of magnitude larger than error induced by the approximation (22). Note that the growth in space of the planar filament scales like $\exp(\alpha V x)$. Both the size of the deflections and the error term $J[\phi, \psi]$ grow in space, but the error term generally remains four orders of magnitude smaller than the deflection size.

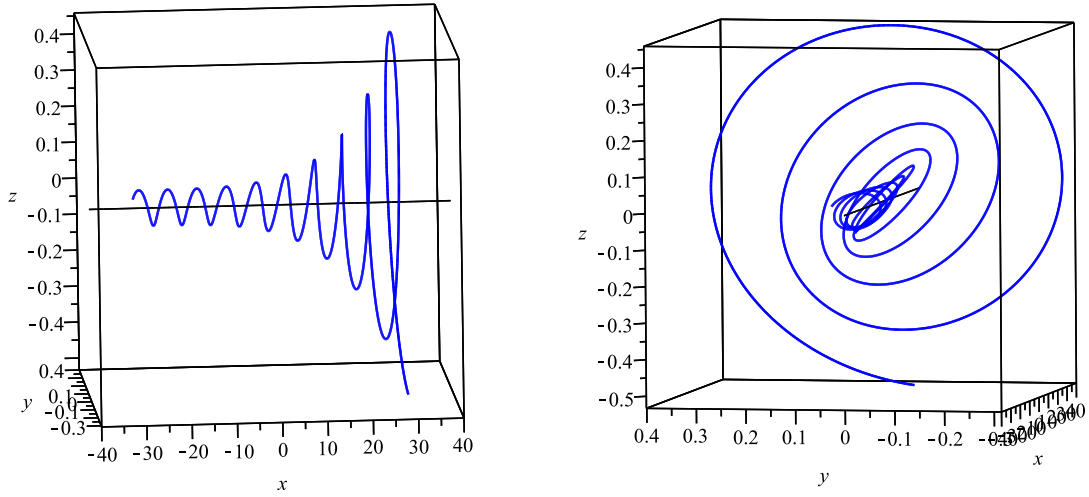


Figure 3: (Color Online) Plot of the deformed planar filament described by (22) when the temperature of the superfluid is $T=1.5\text{K}$ ($\alpha = 0.073$, $\alpha' = 0.018$) and $V = 1$. The filament is given by numerically solving (23)-(24) subject to $\phi(0) = 0.1$, $\psi(0) = 0$, $\phi'(0) = 0$, $\psi'(0) = 0$. The x -axis is given by a solid black line. The behavior is similar to that seen in Fig. 1, although the rate of growth in space is modified due to the larger value of α .

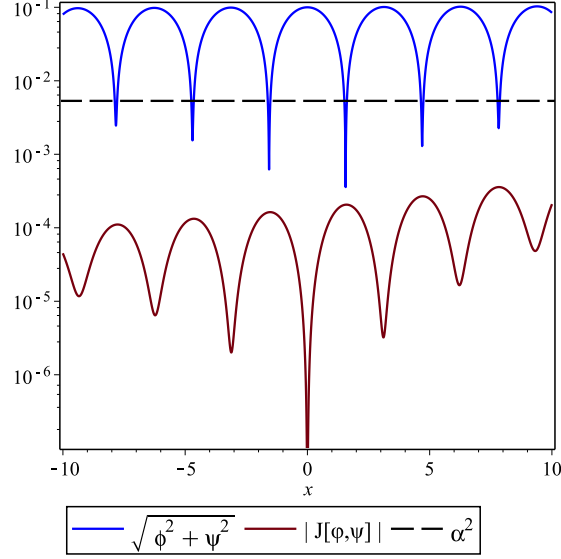


Figure 4: (Color Online) Plot of the error term $J[\phi, \psi]$ over x , along with the norm $\sqrt{\phi^2 + \psi^2}$, for the T=1.5K case. The value of $\sqrt{\phi^2 + \psi^2}$ is a measure of the deviation of the filament from the x -axis. This function again oscillates with a maximal value of the order 10^{-1} , whereas the error due to neglecting non-rotational motion (due to the assumption of a solution of the form (22)) scales near 10^{-4} , and falls below α^2 . This is consistent with the observation that $J[\phi, \psi] = O(\alpha^2)$. To see this, we also plot α^2 for our choice of $\alpha = 0.073$. What this shows is that the magnitude of the deflections from the x -axis are orders of magnitude larger than error induced by the approximation (22). Note that the growth in space of the planar filament scales like $\exp(\alpha V x)$.

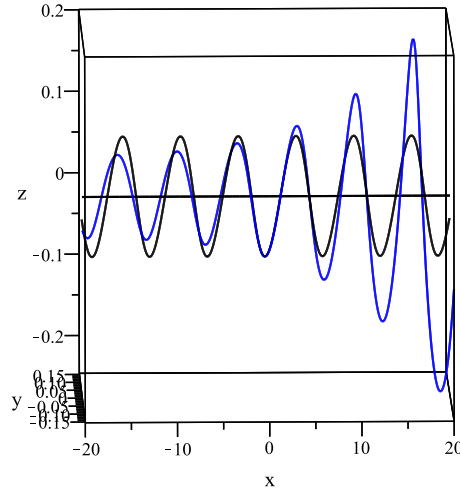


Figure 5: (Color Online) Comparison of the deformed planar filament described by (22) when the temperature of the superfluid is $T=1.5\text{K}$ ($\alpha = 0.073$, $\alpha' = 0.018$) and $V = 1$, along with the classical planar filament corresponding to $\alpha = \alpha' = 0$. In both cases, the filaments are given by numerically solving (23)-(24) subject to $\phi(0) = 0.1$, $\psi(0) = 0$, $\phi'(0) = 0$, $\psi'(0) = 0$. The blue curve represents the $T=1.5$ deformed planar filament, while the black curve represents the classical planar filament.

4 Conclusions

In summary, the quantum planar vortex filament differs from the well-known classical planar vortex filament in some important qualitative respects. First, there is a growth in space of the planar perturbations of the quantum filament along the axis of orientation. This is caused by the normal fluid velocity directed along the filament. Next, while the classical planar filament maintained its form, the extension to the quantum model results in a filament that undergoes torsion effects due to the mutual friction parameters. This causes a bending of the once planar filament the farther removed from $x = 0$ we look. On one end of the filament, this results in an almost helical appearance for the filament. On the other end of the filament, an interesting pattern is formed that exhibits regularity but is not as uniform as a helical structure.

What these results suggest is that a planar vortex filament structure in a superfluid should be a localized structure, in contrast to the classical fluid case, where such a filament maintains its form globally. Due to the effect of mutual friction parameters and the normal fluid velocity, we see that on one side of the reference axis, the filament takes on a helical form far enough away from $x = 0$, whereas on the opposite side of the reference axis the filament undergoes strong growth in space. Near $x = 0$, however, the solution maintains a planar form, even for larger values of the mutual friction parameters or the normal fluid velocity. From this, localized planar structures can exist in a superfluid, even if such structures are no longer global like in the classical LIA.

From the Donnelly - Glaberson instability, we know that helical Kelvin waves along a vortex filament amplify in time. In contrast, the deformed planar filament exhibits growth in space of the perturbations along the line filament. Unlike in the case of the helical perturbations where amplification or de-amplification is global, this spatial growth of the planar filament is local in nature, with a strong dependence on the direction of the normal fluid velocity.

A general mathematical stability analysis, of the type considered in [18] for the classical LIA, is very complicated for the vector equation (3) which includes mutual friction. However, one can study the stability of the present solutions under specific small perturbations, numerically. What one finds is that the present solutions are robust under order $O(\alpha^2)$ perturbations. Therefore, the solutions maintain their spatial structure as time evolves, with the motion being a rotation about the central axis. This is consistent with the planar solutions to the classical LIA. However, note that the approximation (22) neglects motion that is not rotational. This motion occurs at $O(\alpha^2)$ (for the numerical cases we have considered). So, the approximation (22) is valid for sufficiently small α . The error due to such an approximation is shown in Figs. 2 and 4. In the $V \rightarrow 0$ limit, the small $O(\alpha^2)$ error results in a slow spatial growth of the filament, even though one would not be physically expected when $V = 0$. When $V \neq 0$, then the spatial growth is dominated by the $O(\alpha)$ growth discussed above, and the $O(\alpha^2)$ error does not play a strong role.

The classical LIA is obtained from the quantum LIA in the limit $\alpha, \alpha' \rightarrow 0$. This corresponds to the zero-temperature limit. On the other hand, when $T \rightarrow 2.17\text{K}$, the mutual friction parameters become of order unity. In this limit, we are no longer in the perturbative regime, so neglecting non-rotational motion of a filament is no longer feasible. An assumption other than that given in (22) would therefore be required. The present results are most useful in the regime where both α and α' are sufficiently small so that $\alpha^2 \ll \alpha$, which according to [8] is the regime where $T < 2.0\text{K}$. While planar or deformed planar solutions do not appear likely in this limit, other solutions are certainly reasonable. For instance, helical solutions can exist in the “warm” $T \rightarrow 2.17\text{K}$ limit.

In the case where the growth of the deformed planar filament in space is strong (i.e., the warmer

superfluid case), non-local effects will likely play a considerable role in the time evolution of the vortex filament in an unbounded domain. If the filament is confined to a finite spatial domain, there will be a limit to the extent to which the filament will grow in space. In this situation, there will be a segment of the filament which grows in space although the growth will be limited by the size of the domain. However, to more properly model this scenario, non-local effects likely need to be taken into account, since the large amplitude segment of the filament would possibly interact with the boundary of the domain. Therefore, while the spatial growth under LIA is continuous in the direction of the normal fluid flow, realistically any tendency for the amplitude to grow without bound would likely be mitigated by non-local effects once the amplitude was large enough. The first step in studying the non-local effects would be to consider whether planar vortex filament exists under the full Biot-Savart dynamics, which is what the classical LIA approximates. As it turns out, such filaments can actually be shown to exist under the non-local dynamics, and this will be the topic of a forthcoming paper [26].

Acknowledgements

RAV supported in part by NSF grant number # 1144246. The author thanks the reviewers for their helpful remarks, which have improved the quality of the paper.

References

- [1] Landau, L.D. 1941 The theory of superfluidity of helium II. *J. Phys.* **5**, 71.
- [2] Feynman, R.P., 1955 Progress in Low Temperature Physics, Vol. 1, North-Holland, Amsterdam, p. 17.
- [3] Gross, E.P. 1961 Structure of a quantized vortex in boson systems. *Il Nuovo Cimento* **20**, 454-477.
- [4] Hall, H. E. & Vinen, W. F. 1956a The rotation of liquid helium II. I. Experiments on the propagation of second sound in uniformly rotating helium II. *Proc. R. Soc. Lond. A* **238**, 204.
- [5] Hall, H. E. & Vinen, W. F. 1956b The rotation of liquid helium II. II. The theory of mutual friction in uniformly rotating helium II. *Proc. R. Soc. Lond. A* **238**, 215.
- [6] Bekarevich, I. L. & Khalatnikov, I. M. 1961 Phenomenological derivation of the equations of vortex motion in He II. *Sov. Phys. JETP* **13**, 643.
- [7] Nemirovskii, S. K. 2013 Quantum turbulence: Theoretical and numerical problems. *Physics Reports* **524**, 85-202.
- [8] Schwarz, K. W. 1985 Three-dimensional vortex dynamics in superfluid ^4He : Line-line and line-boundary interactions. *Phys. Rev. B* **31**, 5782.
- [9] Landau, L.D. & Lifshitz, E.M. Fluid Mechanics, Addison and Wesley (1959).
- [10] Arms, R.J. & Hama, F.R. 1965 Localized-induction concept on a curved vortex and motion of an elliptic vortex ring. *Phys. Fluids* **8**, 553.

- [11] Da Rios, L.S. 1906 Sul moto d'un liquido indefinite con un filetto vorticoso di forma qualunque. *Rend. Circ. Mat. Palermo* **22**, 117.
- [12] Hasimoto, H. 1971 Motion of a Vortex Filament and its relation to Elastica, *Journal of the Physical Society of Japan* **31**, 293.
- [13] Kida, S. 1981 A vortex filament moving without change of form. *J. Fluid Mech.* **112**, 397.
- [14] Kida, S. 1982 Stability of a steady vortex filament, *Journal of the Physical Society of Japan* **51**, 1655.
- [15] Fukumoto, Y. 1997 Stationary configurations of a vortex filament in background flows, *Proceedings of the Royal Society of London A* **453**, 1205.
- [16] Van Gorder, R.A. 2012 Integrable stationary solution for the fully nonlinear local induction equation describing the motion of a vortex filament, *Theor. Comput. Fluid Dyn.* **26**, 591.
- [17] Van Gorder, R.A. 2013 Scaling laws and accurate small-amplitude stationary solution for the motion of a planar vortex filament in the Cartesian form of the local induction approximation, *Phys. Rev. E* **87**, 043203.
- [18] Van Gorder, R. A. 2013 Orbital Stability for Rotating Planar Vortex Filaments in the Cartesian and Arclength Forms of the Local Induction Approximation. *Journal of the Physical Society of Japan* **82**, 094005.
- [19] Umeki, M. 2010 A locally induced homoclinic motion of a vortex filament. *Theor. Comput. Fluid Dyn.* **24**, 383.
- [20] Van Gorder, R.A. 2012 Exact solution for the self-induced motion of a vortex filament in the arclength representation of the local induction approximation, *Phys. Rev. E* **86**, 057301.
- [21] Van Gorder, R. A. 2012 Fully nonlinear local induction equation describing the motion of a vortex filament in superfluid ^4He . *J. Fluid Mech.* **707**, 585.
- [22] Van Gorder, R. A. 2014 Quantum vortex dynamics under the tangent representation of the local induction approximation. *J. Fluid Mech.* **740**, 5.
- [23] Cheng, D. K., Cromar, W. M. & Donnelly, R. J. 1973 Influence of an Axial Heat Current on Negative-Ion Trapping in Rotating Helium II. *Phys. Rev. Lett.* **31**, 433.
- [24] Glaberson, W. I., Johnson, W. W. & Ostermeier, R. M. 1974 Instability of a Vortex Array in He II. *Phys. Rev. Lett.* **33**, 1197.
- [25] Ostermeier, R. M. & Glaberson, W. I. 1975 Instability of vortex lines in the presence of axial normal fluid flow. *J. Low Temp. Phys.* **21**, 191.
- [26] Van Gorder, R. A. 2014 Non-local dynamics of the self-induced motion of a planar vortex filament, submitted.